Physicochem. Probl. Miner. Process., 60(5), 2024, 193459

http://www.journalssystem.com/ppmp

Physicochemical Problems of Mineral Processing

ISSN 1643-1049

Recovering rare earth elements from svanbergite ores by roasting and phosphoric acid leaching

Keyu Ma [1,2,3], Jie Zhang [1], Pengpeng Men [4], Qiufeng Deng [5], Jun Rao [2,3]

[1] Collage of Mining, Guizhou University, Guiyang 550025, China; 380425852@qq.com

[2] Engineering Research Center for Silicate Solid Waste Resource Utilization of Hebei Province, HeBei GEO University, Shijiazhuang 510000, China

[3] Hebei Key Laboratory of Green Development of Rock Mineral Materials, HeBei GEO University, Shijiazhuang 510000, China

[4] North Engineering Design and Research Institute Co., Ltd., Shijiazhuang 510000, China

[5] Guizhou Tianbao Mineral Resources Consulting Service Co., Ltd., Guiyang 550000, China

Corresponding author: jzhang@gzu.edu.cn (Jie Zhang)

Abstract: Rare earth elements (REEs) are regarded as key global strategic metals, and recovering REEs from phosphate ores might constitute an alternative method of acquiring rare earth resources. Svanbergite ores in Sichuan are particular phosphates rocks that contain abundant REEs, which are valuable resources that have not been fully developed and utilized. Consequently, the development of crucial technologies for extracting REEs from svanbergite ores hold strategic and scientific significance. This study employed roasting and phosphoric acid leaching processes to recover REEs from svanbergite ores. Response surface methodology (RSM) was applied to optimize the hydrometallurgical process parameters. This study found that the optimal conditions for REEs recovery were: a roasting temperature 600℃, a roasting time of 38.72 min, a phosphoric acid concentration of 40%, a leaching liquid/solid mass ratio of 10, a leaching temperature of 75℃ and a leaching time of 70 min, resulting in a maximum predicted REE recovery rate of 83.57%. The experimental values exhibited a high degree of proximity to the predicted values, thereby substantiating the accuracy of the model and validating the plausibility of the optimized solution. Mechanistic analysis revealed that after the roasting process, the crandallite formed new acid-soluble new phases. Following the phosphoric acid leaching process, REEs were present predominantly in the form of REE^{3+} in the leaching solution, consequently separating the REEs from the svanbergite ores. This study provides a valuable reference for the recovery of REEs from associated rare earth phosphate ores.

***Keywords*:** rare earth elements, svanbergite, response surface methodology, roasting, phosphoric acid

1. Introduction

Rare earth elements, strategic key metals with outstanding properties and wide application in various emerging fields, play a vital and irreplaceable role in social development and national security (Cheng and Che, 2010; Huang et al., 2011; Weng et al., 2015). The total amount of phosphate ore associated with REEs worldwide, which is as high as 10 billion tons with an average grade of 0.05% of REEs, is expected to become an important supplement to traditional rare earth mineral resources. However, due to the limitations of REE occurrence, crystal structure, and technological level, the process of recovering REEs from phosphate minerals has not reached levels required for industrialization (Zheng et al., 2017; Liang et al., 2017). Consequently, the development of key technologies for extracting phosphorus-based REEs will lead to paths for the development of rare earth resources (Group, 2019).

Svanbergite ore, which is a rare type of phosphate ore, is mostly distributed in Mianzhu City and Shifang City in Sichuan Province, China (Duan et al., 1964; Sun, 1966). The ore mainly consists of phosphorus and includes several useful components, including aluminium, strontium, and rare earth. Notably, the rare earth content of svanbergite ore is higher than that of the general phosphate rocks

DOI: 10.37190/ppmp/193459

(Tang et al., 1982; Wang and Xia, 1988; Ma et al., 2022). Previous studies have focused mostly on the recovery of REEs from yellow phosphorus slag, whereas there has not been a systematic investigation of REE recovery in the hydrometallurgical processes (Huang, 1977; Li, 1078; Huang and Tang, 1987). Despite the relatively stable chemical properties of svanbergite ore（Wang et al., 1986; Wang, 1991）, it is easily soluble in acid after roasting, which serves as the basis for wet processing and utilization (Huang, 1985; Yu et al., 2008).

The REE content associated with phosphate ore is relatively low, and flotation is typically employed to increase the grade of REEs (Zhang et al., 2003; Jin et al., 2008; Al-Thyabat and Zhang, 2016; Feng et al., 2024). Then, REEs are recovered from flotation phosphate concentrate via thermal or wet processes, among which the wet process is relatively mature and widely employed. Presently, common wet processing methods for extracting REEs from phosphate ore include the H2SO4 method, HNO_3 method, HCl method, and H_3PO_4 method (Monir et al., 1999; Wu et al., 2018; Battsengel et al., 2018; Amine et al., 2019). The H_2SO_4 method is the main treatment process, requiring additional processes for recovering REEs from phosphoric acid and phosphogypsum (Wu et al., 2015). The H_3PO_4 method enriches REEs into leaching solution without introducing extra ion impurities into the leaching system (Wang, 2018; Wu et al., 2019; Li et al., 2021).

Response surface methodology (RSM) is an analytical optimization approach based on experimental design, model construction, and data analysis, with the aim of assessing the interactions among factors and determining the optimal experimental conditions. Box Behnken designs (BBD) and centre composite designs (CCD) are the most commonly utilized experimental design and statistical analysis methods in second-order response surface design (Salehi et al., 2015; Li et al., 2023). Because of its advantages, including fewer experiments, high accuracy of the regression model, strong predictive performance, and good visualization effect, RSM has been widely applied in various fields (Hamzaoui et al., 2008; Li et al., 2015).

On the basis of previous research achievements, this study focuses on svanbergite and has established a new wet extraction process for REEs, which employs roasting for the preactivation of the raw svanbergite, with the aim of creating new substances that can readily release REEs. Subsequently, REEs are extracted from roasted ores with a phosphoric acid solution, which results in high leaching efficiency, does not introduce additional impurity ions in the leaching system, and enriches REEs in the leaching solution. Moreover, the recycling of phosphoric acid may also be accomplished for subsequent utilization. RSM was employed to optimize the process conditions and determine the optimal extraction conditions of the roasting–leaching process, aiming to maximize REE recovery. These research outcomes can establish a technical basis for the comprehensive wet utilization of rare earth-containing svanbergite ore and may provide a novel process for the development and utilization of phosphorus-based rare earth resources.

2. Materials and methods

2.1. Experimental materials and apparatus

2.1.1. Experimental materials

In this study, the raw svanbergite ores samples from northwestern Sichuan, China, were successively crushed to sizes of less than 2 mm with a jaw crusher (PEX–100×125, Wuhan Hengle Mineral Engineering Equipment Co., Ltd) and a roll crusher screening machine (XPS–Φ250×150, Wuhan Hengle Mineral Engineering Equipment Co., Ltd). The crushed samples were subsequently ground to diverse particle sizes via a sealed laboratory sample preparation mill (GJ100-3, Bangxi Instrument Technology (Shanghai) Co., LTD). The comminuted samples were subjected to chemical and mineral analysis, synchronous thermal analysis and REE roasting-leaching experiments. Additionally, representative block ores were selected to grind electron probe slices for Laser Ablation Inductively Coupled Plasma Mass Spectrometry (LA–ICP–MS, GeolasPro 193nm laser ablation system + Agilent 7900 mass spectrometer).

Phosphoric acid solutions (mass fraction, %) were prepared by diluting concentrated phosphoric acid (AR, Tianjin Oubokai Chemical Co., Ltd). The water used in this experiment was prepared with an ultrapure water treatment system (TST, Shijiazhuang Tester Instrument Co., Ltd).

2.1.2. Analytical apparatus

The chemical compositions were measured via X–ray fluorescence spectrometry (P61–XRF26s). The mineral compositions and the leaching residues were analysed with an automatic mineral analysis system (MLA650, Hardware: Sigma 500 field emission scanning electron microscope (SEM), Zeiss, Germany, Quantax double probe energy spectrometer, Brook, Germany, Software: AMICS mineral automatic dissociation System, Brook, Germany) and an X–ray diffractometer (XRD, Rigaku Ultima IV, Japan, Test target material: copper target, scanning angle: 10 to 80 degrees, scanning speed: 2°/min). REE concentrations in the leaching solutions were determined via inductively coupled plasma–mass spectrometry (ICP–MS, ICAP QC, Thermo fisher). The quality changes and thermal effects of the svanbergite ore during the heating process were measured via a synchronous thermal analyser (TG–DSC, NETZSCH STA 409 PC, German Nike company, 5K/min, 30–1000℃).

2.2. Mineralogical analysis

2.2.1. Chemical compositions

Chemical analysis (in Table 1) reveals that svanbergite ore is composed mainly of P_2O_5, Al_2O_3, CaO, SrO, SO_3, and Fe_2O_3 as medium-grade phosphate ore. The REE content is 0.25% (2080.35 μg/g), which can be fully recovered for high ore value-added utilization.

2.2.2. Mineral compositions

The mineralogical composition (Figs. 1 & 2) shows that the svanbergite ores mainly comprise crandallite, pyrite, apatite, and clay. The AMICS analysis results also indicate that the mineral composition is complex and closely related. Crandallite which is a calcium aluminium phosphate mineral with strong cation exchange ability, is the main valuable mineral. Ca^{2+} and H^+ can be replaced by REE^{3+} (Fig. 14), and Ca^{2+} can be substituted by Sr^{2+} (Rloand et al., 2000). LA–ICP–MS analysis revealed that crandallite contains a large amount of REEs.

Table 1. Chemical multi-element analysis of svanbergite ore (XRF) (wt%)

Oxides	Al_2O_3	CaO	TFe_2O_3	P_2O_5	SiO_2	SO_3	SrO
Assay Value	26.11	7.64	14.81	21.70	0.83	28.40	4.81
Oxides	MgO	BaO	K_2O	TiO_2	ZrO_2	MnO	REEs
Assay Value	0.08	0.31	0.08	1.32	0.13	0.01	0.25

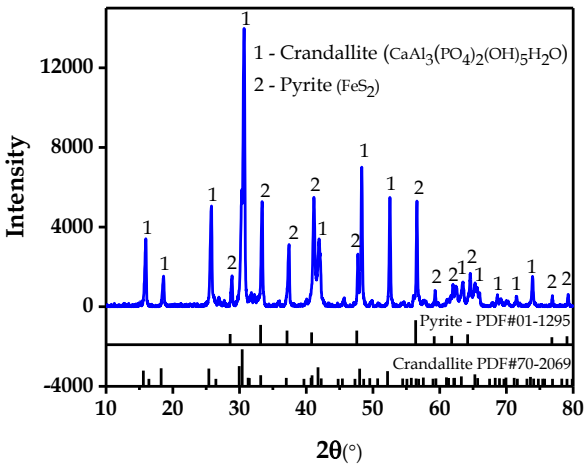

Fig. 1. XRD analysis of raw svanbergite ores

Fig. 3 also shows that the distribution area of Sr is exactly consistent with those of Al, Ca, and P. It is speculated through the above analysis that REEs and Sr mainly exist in crandallite. Pyrite is the main gangue mineral, and both apatite and clay have low contents. These minerals are closely embedded and mainly dispersed in crandallite as fine particles (less than 30 μm).

On the basis of the above analysis, crandallite is a vital target mineral for the experimental recovery of REEs. Considering the complex mineral relationships and fine-grained distribution characteristics, this study adopted roasting acid leaching to recover REEs.

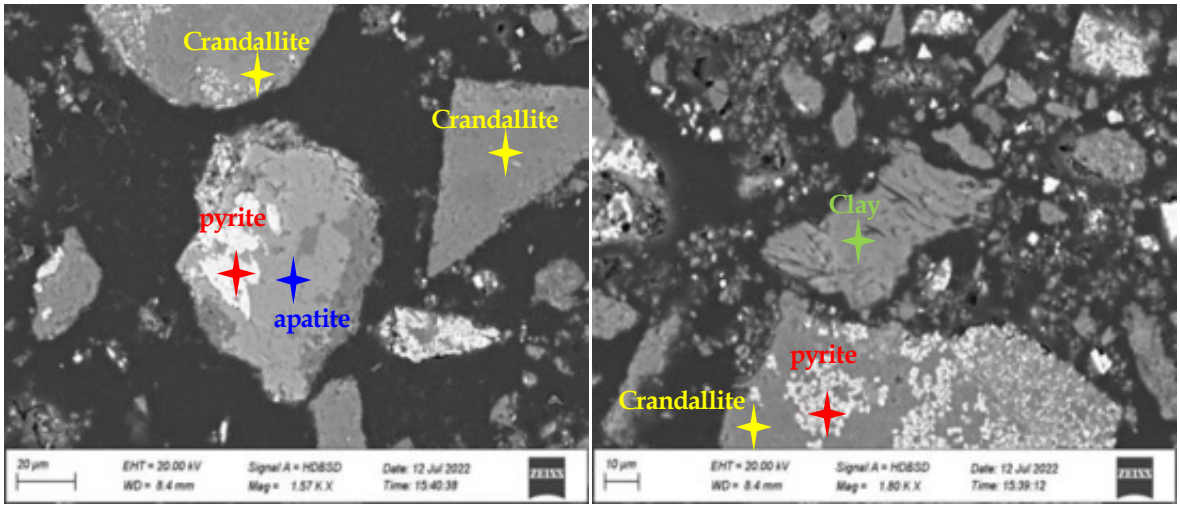

Fig. 2. BSE images of AMICS analysis

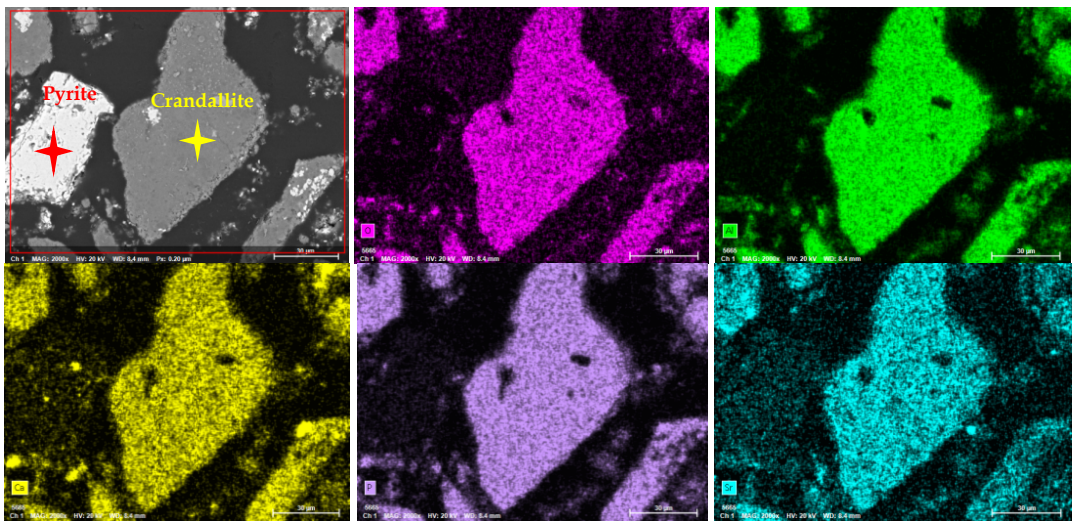

Fig. 3. AMICS analysis (BSE image and elemental distribution maps of crandallite)

2.3. Experimental methods and design

2.3.1. Experimental procedure

The -125 μm samples are roasted within a chamber electric furnace (SX–4–10, Tianjin tester Instrument Co., Ltd), and then used for leaching tests. The detailed leaching operations were as follows: the roasted ores were dissolved in diluted phosphoric acid via a magnetic stirring in an electric thermostatic water bath (HCJ–E, Changzhou Enpei Instrument Manufacturing Co. LTD), the leaching solutions were filtered with a circulating water multipurpose vacuum pump (SHI–D(III), Gongyi City Yingyu high-tech instrument factory), the REE concentrations in the filtrate were measured via ICP–MS, and the residues were analysed via X–ray diffraction (XRD).

2.3.2. Calculation of leaching rate

Leaching recovery is applied to evaluate the leaching effectiveness of REEs, and the higher the value is, the finer. The leaching recoveries of the REEs were calculated via Formula (1).

$$\varepsilon = \frac{c_1 \times v_1}{\omega_0 \times m_0} \times 100\% \quad (1)$$

where ε represents the leaching recovery of REEs, %; v1 represents the volume of the leaching solution, mL; c1 represents the concentration of REEs in the leaching solution, μg/mL; ω0 represents the REEs content in the raw ore, μg/g; m0 represents the mass of the raw ore, g.

2.3.3. Experimental design

Central composite design (CCD) was applied in roasting and leaching experiments, and the optimal roasting–leaching process conditions were predicted by analysing the experimental data and response surfaces with Design Expert software (version 8.0.6, Stat Case, Inc, Minneapolis, MN, USA). Table 2 presents the codes and levels of roasting variables, where the roasting temperature (℃) and time (min) are represented by the independent variables Ar and Br, respectively, and the REE leaching recovery ε R (%) is the response value.

Table 2. Code and level of roasting experiment factors

Factor	Unit	Code	Level				
			-1.414	-1	0	1	1.414
Temperature	℃	A_r	431.01	460	530	600	628.99
Time	min	B_r	8.79	15	30	45	51.21

Table 3. Code and level of leaching experiment factors

Factor	Unit	Code	Level				
			-2	-1	0	1	2
Acid concentration	%	A	25	30	35	40	45
Liquid- solid ratio（L/S）	—	B	4	6	8	10	12
Temperature	℃	C	30	45	60	75	90
Time	min	D	10	30	50	70	90

The leaching variables (Table 3) include the acid concentration A (%), liquid–solid mass ratio B, leaching temperature C (℃), and leaching time D (min), and their centre values are 35%, 8, 60℃, and 50 min respectively, with the REE leaching recovery εL (%) being the response value.

3. Results and discussion

3.1. Model establishment and analysis of variance for roasting pre-activation

Thirteen roasting experiments were performed, and the leaching conditions included an acid concentration of 30%, a liquid–solid mass ratio of 8, a leaching temperature of 30℃, and a leaching time of 30 min. The experimental results (Table 4) and errors (Fig. 4) indicate that the REE leaching recoveries under different experimental conditions ranged from 17.94% to 80.86%.

Table 4. CCD and results for roasting experiment

No.	A_r(℃)	B_r (min)	REEs (%)
1	460	15	17.94
2	600	15	69.99
3	460	45	27.73
4	600	45	80.59
5	431.01	30	23.35
6	628.99	30	80.86
7	530	8.79	31.15
8	530	51.21	56.93
9	530	30	59.09
10	530	30	60.1
11	530	30	58.31
12	530	30	52.17
13	530	30	55.75

3.1.1. Response surface regression analysis

Through the application of quadratic multiple regression fitting and variance analysis to the experimental roasting data, the established multiple quadratic regression equation is shown in Eq. (2).

$$\varepsilon_R\ (\%) = 57.08 + 23.28A + 7.11\ B + 0.20AB - 2.24A^2 - 6.27B^2 \quad (2)$$

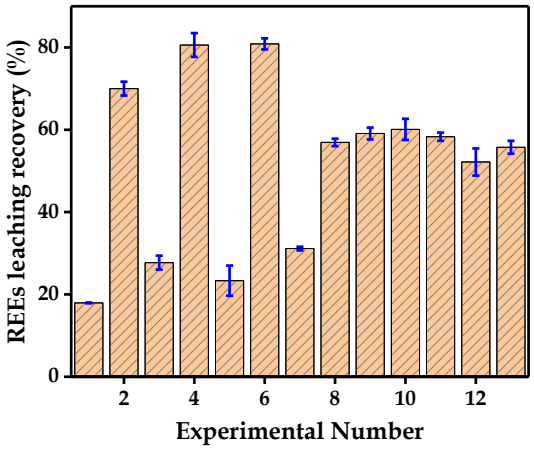

Fig. 4. Errors in roasting experiment data

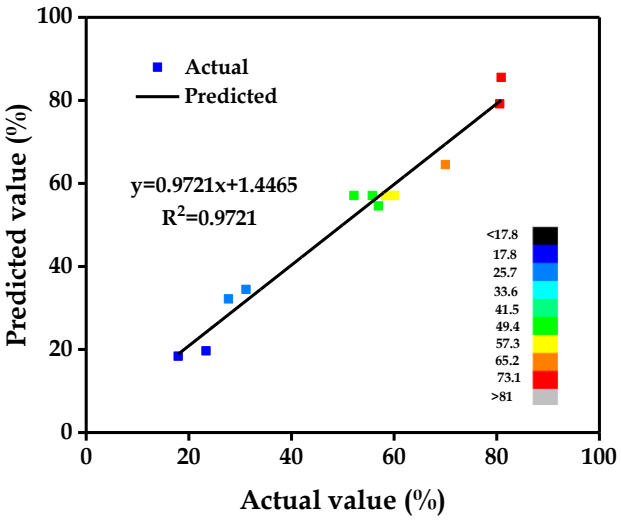

Fig. 5. Comparison of predicted and actual value of REEs leaching recovery for roasting experiment

Fig. 5 shows the comparison chart between the actual values and the model-predicted values of REE leaching recovery in the roasting experiment. The diagonal line represents the agreement of between the actual value and the predicted value. The actual values are all around the diagonal line, indicating a good fit between the model and the actual data.

3.1.2. Variance analysis of the model

The results of the variance analysis for the roasting experiment are presented in Table 5. The significance of the factor could be judged on the basis of the P value, where $P < 0.05$ indicates significance, and $P < 0.001$ indicates extreme significance. It is clearly observable that the model $P < 0.0001$, the lack of fit $P = 0.1334 > 0.05$, and $R2 = 0.9721$. This indicates that the model is statistically significant and has a considerable level of fitness. Both A and B are significant factors, and the sequence of significance is A > B, which demonstrates that the impact of roasting temperature on the leaching of REEs is more pronounced than that of roasting time. Furthermore, the interaction between A and B is not significant, and that the impact of the quadratic term A2 is also not significant. However, B2 has a notable effect on the leaching of REEs.

Table 5. Variance analysis for roasting experiment

Source	Sum of Squares	df	Mean Square	F-value	p-value
Model	5028.08	5	1005.62	48.79	<0.0001*
A- Reaction temperature (℃)	4335.73	1	4335.73	210.36	<0.0001*
B- Reaction time (min)	403.97	1	403.97	19.60	0.0031*
AB	0.16	1	0.16	7.958E-003	0.9314
A^2	34.97	1	34.97	1.70	0.2340
B^2	273.87	1	273.87	13.29	0.0082*
Residual	144.28	7	20.61		
Lack of Fit	103.73	3	34.58	3.41	0.1334
Pure Error	40.55	4	10.04		
Cor Total	5172.36	12			

3.1.3. Interaction between factors and response surface analysis

The contour and response surface graphs (Fig. 6) that are based on the regression equation illustrate the influences of roasting temperature and time on the leaching recoveries of REEs. These findings demonstrate that the that roasting temperature plays a positive role in the extraction of REEs. The REE leaching recoveries are relatively low when the temperature is below 430℃, indicating that minerals with REEs are not easily destroyed below this temperature. the REE leaching recoveries significantly increase when the temperature increases to 530°C, demonstrating that high temperatures can destroy the structure of minerals and facilitate the REE release. Furthermore, phase transformation can be accomplished within a relatively short period. Higher roasting temperature results in greater amounts of energy absorbed per unit mass of ore, shorter the time required for the destruction of mineral functional groups, and quicker the formation of new phases.

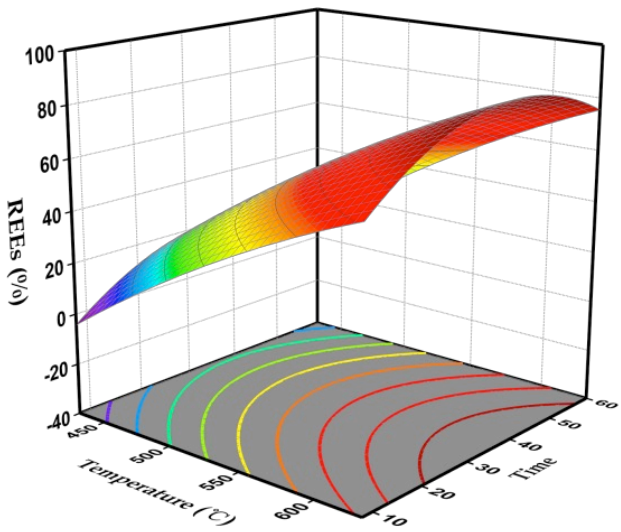

Fig. 6. Effect of roasting temperature and time on the leaching recovery of REEs (125μm, 30% acid concentration, L/S ratio 8, 30℃, 30min, 300 r/min)

3.1.4. Optimum process conditions and model validation

The predicted optimal roasting conditions and results are presented in Table 6. The optimal roasting conditions involved a roasting temperature of 600°C, a roasting time of 38.72 min and a predicted REE leaching recovery of 80.25%. To validate the accuracy of the prediction, repeated experiments were carried out under the optimal modified conditions. The experimental REE recovery rate (81.75%) is relatively close to that of the predicted results, which demonstrates that the response surface model is precise and that the predicted outcomes are dependable.

Table 6. Comparison of the predicted and leaching recovery rate under optimal roasting process conditions

Roasting experiment		leaching experiment				Experimental value	Predicted value	Desirability
A_r	B_r	A (%)	B (g/g)	C (℃)	D(min)	REEs (%)	REEs (%)	
600	38.72	30	8	30	30	81.75	80.25	0.995

3.2. Model establishment and analysis of variance for leaching

The conditions and results of the leaching experiment are presented in Table 7, and the errors in the test data are shown in Fig. 7. Thirty leaching experiments were performed at 600℃ and 38.75 min, and the recoveries of REEs reached 83.89%.

Table 7. CCD and results for leaching experiment

No.	A (%)	B (g/g)	C (℃)	D (min)	REEs (%)
1	30	6	45	30	68.91
2	40	6	45	30	61.94
3	30	10	45	30	81.32
4	40	10	45	30	80.92
5	30	6	75	30	65.94
6	40	6	75	30	75.48
7	30	10	75	30	73.07
8	40	10	75	30	82.06
9	30	6	45	70	67.39
10	40	6	45	70	78.63
11	30	10	45	70	79.76
12	40	10	45	70	76.66
13	30	6	75	70	63.44
14	40	6	75	70	73.8
15	30	10	75	70	77.42
16	40	10	75	70	82.46
17	25	8	60	50	70.41
18	45	8	60	50	83.89
19	35	4	60	50	59.42
20	35	12	60	50	78.69
21	35	8	30	50	82.58
22	35	8	90	50	74.89
23	35	8	60	10	75.63
24	35	8	60	90	75.63
25	35	8	60	50	77.54
26	35	8	60	50	78.8
27	35	8	60	50	79.06
28	35	8	60	50	71.98
29	35	8	60	50	72.16
30	35	8	60	50	75.08

3.2.1. Response surface regression analysis

The regression equation for the leaching experiments is presented in Eq. (3).

$$\varepsilon_L\ (\%) = 76.34 + 2.57A + 4.86B - 0.72C + 0.41D - 0.85AB + 2.07AC + 0.77AD - 1.89B^2 \quad (3)$$

A graph of the relationship between the actual and predicted values of REEs recovery for the leaching experiment is shown in Fig. 8. The model clearly fits relatively well with the experimental data.

3.2.2. Variance analysis of the model

Table 8 lists the variance analysis outcomes of the leaching experiments. The model has a P value of less than 0.0001, whereas the lack of fit has a P value of 0.4589, which is greater than 0.05. Additionally, the R2 value is 0.7920, confirming that the model is significant and valid. The F values revealed that REE recovery was most significantly affected by the acid concentration and the liquid–solid ratio, whereas the leaching temperature and leaching time were less significant. In addition, there is a notable interaction between the acid concentration and leaching temperature, and the leaching of REEs is also considerably impacted by the square of the liquid–solid ratio.

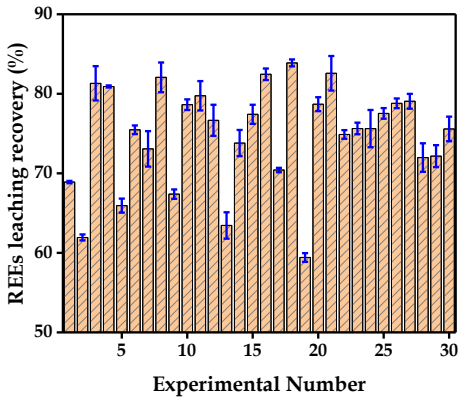

Fig. 7. Errors in leaching experiment data

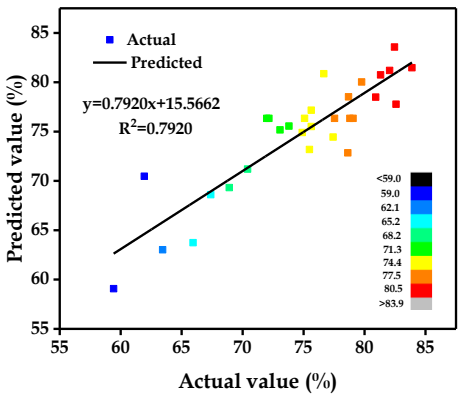

Fig. 8. Comparison of predicted and actual value of REEs leaching recovery for leaching experiment

Table 8. Variance analysis for leaching experiment

Source	Sum of Squares	df	Mean Square	F-value	p-value
Model	934.57	8	116.82	9.99	<0.0001*
A-Acid concentration (%)	158.41	1	158.41	13.55	0.0014*
B-liquid–solid ratio	567.26	1	567.26	48.53	<0.0001*
C-Temperature (℃)	12.38	1	12.38	1.06	0.3150
D-Time (min)	4.10	1	4.10	0.35	0.5600
AB	11.63	1	11.63	0.99	0.3299
AC	68.72	1	68.72	5.88	0.0244*
AD	9.58	1	9.58	0.82	0.3756
B^2	102.48	1	102.48	8.77	0.0075*
Residual	245.47	21	11.69		
Lack of Fit	194.46	16	12.15	1.19	0.4589*
Pure Error	51.01	5	10.20		
Cor Total	1180.04	29			

3.2.3. Interaction between factors and response surface analysis

3.2.3.1. Effect of acid concentration and liquid–solid ratio on the leaching recovery of REEs

The contour and response surface plots in Fig. 9 for the leaching experiment indicate the effects of acid concentration and liquid–solid ratio on REE recovery. When the liquid–solid ratio increases, the REE leaching recovery significantly increases, demonstrating that the liquid–solid ratio has a considerable effect on the REE leaching, and that this effect is more pronounced under lower acidity conditions.

The liquid–solid ratio is positively correlated with the amount of leaching agent used and negatively correlated with the viscosity of the leaching solution system, which affects the REE leaching efficiency and the complexity of the subsequent treatment process. That is, an increase in the liquid–solid ratio can increase the amount of phosphoric acid and decrease the viscosity of the solution, which is beneficial for the stirring, transportation, and solid–liquid separation, resulting in a higher leaching efficiency of the REEs. Nevertheless, if the liquid–solid ratio is too high, the consumption of the phosphoric acid solution increases, causing the REE concentration in the leaching solution to decrease, which is not favourable for REE extraction and increases the quantity of leachate to be treated.

The acid concentration is also a significant factor that affects REE leaching recovery. The lower the liquid–solid ratio is, the more pronounced the effect of the acid concentration. When the liquid–solid ratio is relatively small, high REE leaching recovery can be obtained under high acid concentrations, which may lead to environmental risks and safety issues. Thus, the liquid–solid ratio can be properly increased to decrease the concentration of acid.

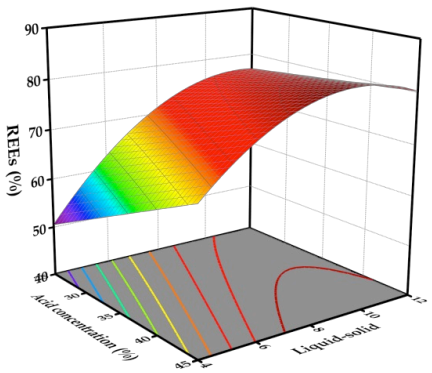

Fig. 9. Effect of acid concentration and liquid–solid ratio on the leaching recovery of REEs (T = 60°C, t = 50min)

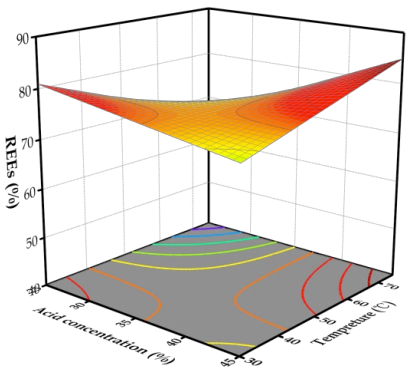

Fig. 10. Effect of acid concentration and temperature on the leaching recovery of REEs (L/S = 8, t = 50min)

3.2.3.2. Effects of acid concentration and temperature on the leaching recovery of REEs

The interaction between acid concentration and temperature is presented in the Fig. 10. The impact of temperature on REE leaching varies with acidity.

In the case of low acidity, as the temperature increases, the REE leaching recovery actually diminishes. This may be due to the weakening of the phosphate ionization process as the temperature rises (Cetiner et al., 2005), along with the reduction in the Gibbs energy of the precipitation reaction of rare earth phosphate ($REPO_4$) (Cetiner, 2003).

Research findings have demonstrated that within phosphoric acid, the primary factor influencing the solubility of rare earth elements (REEs) is the concentration of hydrogen ions [c(H^+)]. The solubility of REEs increases with increasing concentration of phosphoric acid (Wu et al., 2018). Despite the fact that raising the temperature can lower [c(H^+)], in high-acidity phosphoric acid solutions possess an adequate amount of H^+, and thus, a relatively high leaching recovery rate of REEs can still be attained under the conditions of high acidity and high temperature.

This implies that the interaction between the acid concentration and the leaching temperature is significant, and both low temperature with low acidity and high temperature with high acidity, are beneficial for the leaching of REEs. In production, while ensuring a high REE recovery rate, proper acidity and leaching temperature should be selected while considering factors such as energy conservation and economic costs.

3.2.3.3. Effect of acid concentration and time on the leaching recovery of REEs

Fig. 11 presents the effects of acid concentration and time on the leaching recovery of REEs. This reveals that under low acidity, the REE recovery rate slightly decreases with increasing leaching time. The analysis results in (2) suggest that REEs gradually form precipitates under low acidity and high temperature (T = 60℃), causing the REE recovery rate to gradually decrease. Under high-acidity conditions, with sufficient reactants, an increase in leaching time is favourable for REE leaching.

3.2.3.4. Effects of the liquid–solid ratio and temperature on the leaching recovery of REEs

The effects of liquid–solid ratio and temperature on the leaching recovery of REEs are presented in Fig. 12. Under different liquid–solid ratios, the REE recovery rate decreases uniformly with increasing leaching temperature. As stated in (2), under low acidity (C = 35%), increasing the temperature is not beneficial for the leaching of rare earths. When the leaching temperature remains unchanged, the leaching rate increases with increasing liquid–solid ratio. On the basis of the above analysis, the interaction between the liquid–solid ratio and leaching temperature is not remarkable.

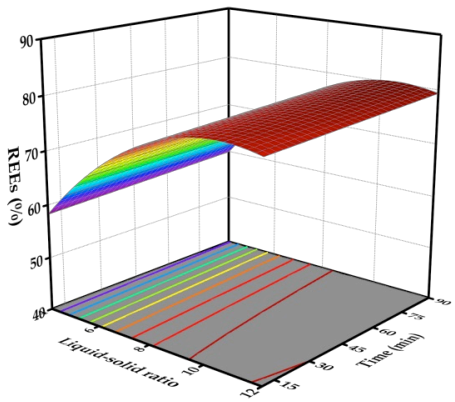

Fig. 13. Effect of liquid–solid ratio and time on the leaching recovery of REEs (C = 35%, T = 60℃)

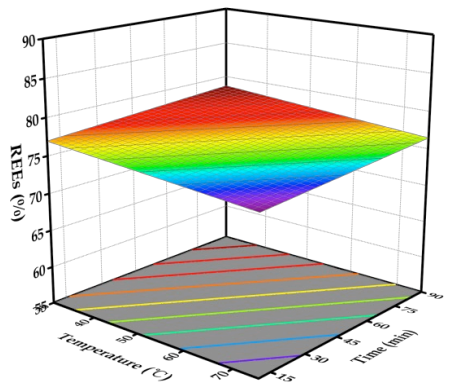

Fig. 14. Effect of temperature and time on the leaching recovery rate of REEs (C = 35%, L/S = 8)

3.2.3.5. Effect of the liquid–solid ratio and time on the leaching recovery of REEs

The effects of the liquid–solid ratio and time on the leaching recovery of REEs are displayed in Fig. 13. Under different liquid–solid ratios, the REE recovery rate increases with increasing leaching time. While the leaching time remains unchanged, the REE recovery rate increases as the liquid–solid ratio increases. This finding reveals that the interaction between the liquid–solid ratio and leaching time is also not of great significance.

3.2.3.6. Effects of temperature and time on the leaching recovery of REEs

Fig. 14 shows the interactive effect of the leaching time and leaching temperature on the leaching recovery of REEs is shown. This shows that the REE recovery rate decreases somewhat as the leaching temperature increases, and gradually increases with increasing leaching time, thus there is no obvious interaction between the liquid–solid ratio and leaching time.

3.2.4. Optimum process conditions and model validation

Table 9 displays the optimal leaching circumstances and outcomes. Under optimal conditions, the predicted and verified values of REE recovery are 83.57% and 82.46%, respectively, with a small error, indicating that the model is precise and that the predicted results are dependable.

Table 9 Comparison of the predicted and leaching recovery rate under optimal roasting-leaching process conditions

Roasting experiment		leaching experiment				Experiment alvalue	Predicted value	Desirability
A_r	B_r	A (%)	B (g/g)	C (℃)	D(min)	REEs (%)	REEs (%)	
600	38.72	40	10	75	70	82.46	83.57	0.99

4. Analysis of the roasting-leaching process

4.1. Analysis of the roasting process

Fig. 15 presents the TG-DSC analysis results for the raw ores. This reveals that the weight gradually decreases when the temperature increases. The removal of free water from the minerals caused a decrease in weight at 115.4℃. There is a weight decrease peak on the DTG curve and a clear exothermic peak on the differential heating curve at 428.6℃, which may be related to the exothermic oxidation of minerals. The weight decreases significantly at 527.8℃, which may be due to the main mineral bond dissociation, indicating that the mineral structures are disrupted and that volatile matter is removed. Above 600℃, the ore weight reduction rate slows down, indicating an insignificant phase transition and gradual stabilization of the new phase crystal structure.

Fig. 16 shows the XRD patterns of the ore samples at various temperatures, which implies that the minerals experienced distinct phase transformations as the temperature fluctuated. Oxidized iron is generated at 431℃, indicating that pyrite undergoes oxidation desulfurization and releases heat at this temperature. Aluminium phosphate, aluminium oxide, and calcium phosphate were formed between 530℃ and 600℃, which clearly indicates that the hydroxyl groups of crandallite were broken down and underwent dehydration, while new phases were generated simultaneously. There was no change in the types of new phases at 700℃, but the peak intensities of each phase increased, which confirms that the crystal structure of the new phases gradually stabilized.

On the basis of the TG-DSC and XRD analyses along with thermodynamic data calculations, it can be concluded that the main roasting reactions are as follows:

$$2FeS_2 + 5.5O_2\,(g) = Fe_2O_3 + 4SO_2\,(g) \quad (4)$$

$$3CaAl_3(PO_4)_2(OH)_5H_2O = Ca_3(PO_4)_2 + 4AlPO_4 + 2.5Al_2O_3 + 10.5H_2O\,(g) \quad (5)$$

$$2SrO + 2SO_2\,(g) + O_2\,(g) = 2SrSO_4 \quad (6)$$

4.2. Analysis of leaching process

The XRD patterns of the samples before and after roasting-leaching are shown in Fig. 17. A comparison of the phases before and after roasting-leaching revealed that the peaks of aluminium phosphate,

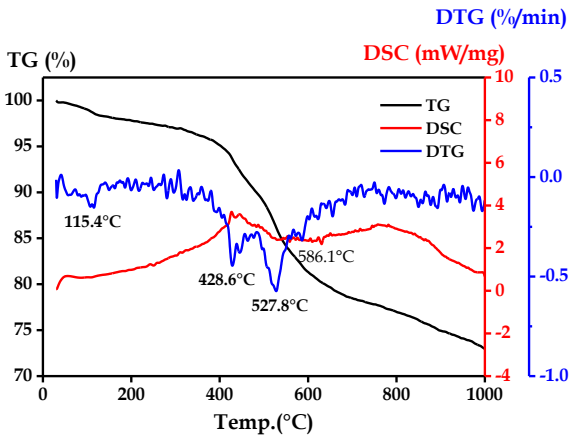

Fig. 15. TG-DSC analysis of samples

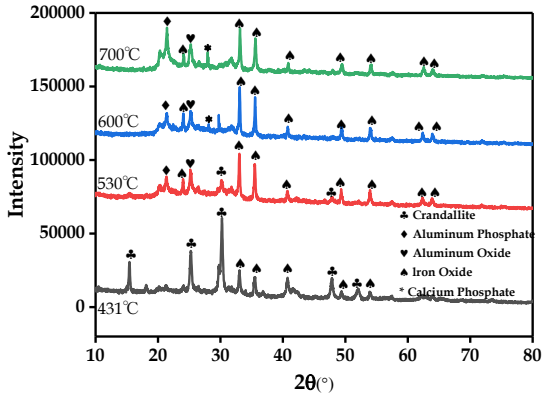

Fig. 16. XRD pattern of samples at different roasting temperatures

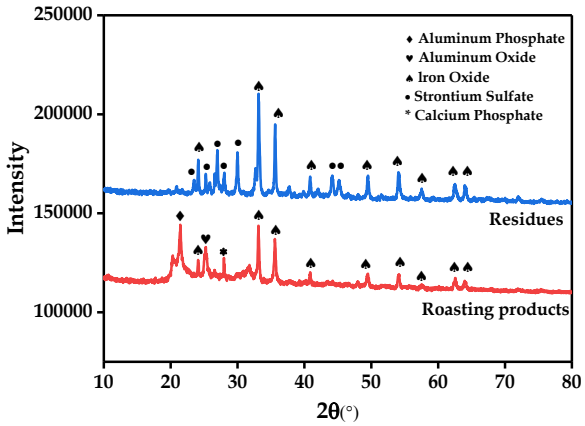

Fig. 17. XRD pattern of samples before and after roasting-leaching

aluminium oxide, and calcium phosphate in the leaching residue disappeared, indicating that they entered the solution during leaching. However, the iron oxide and strontium sulfate remained in the leaching residue.

Phosphoric acid can dissolve insoluble minerals by forming water-soluble complexes with metal ions through dihydrogen phosphate after hydrolysis to promote the dissolution of minerals (Zhang et al., 2021). At room temperature and pressure, phosphoric acid solution mainly contains phosphoric acid (H_3PO_4) and dihydrogen phosphate ions ($H_2PO_4^-$), ensuring the coordination of metal ions and providing the basis for REE separation. When the calcination product reacts with phosphoric acid, Al^{3+}, Ca^{2+}, and RE^{3+} can all chelate with dihydrogen phosphate to form soluble dihydrogen phosphate complexes.

The reactions possible during the leaching are as follows:

$$Ca_3(PO_4)_2(s) + 4H_3PO_4(aq) = 3Ca(H_2PO_4)_2(aq) \quad (7)$$

$$AlPO_4(s) + 2H_3PO_4(aq) = Al(H_2PO_4)_3(aq) \quad (8)$$

$$Al_2O_3(s) + 6H_3PO_4(aq) = 2Al(H_2PO_4)_3(aq) + 3H_2O(aq) \quad (9)$$

$$REPO_4(s) + 2H_3PO_4(aq) = RE(H_2PO_4)_3(aq) \quad (10)$$

According the above analysis, the main phase changes in the roasting and phosphoric acid leaching are presented in Fig.18.

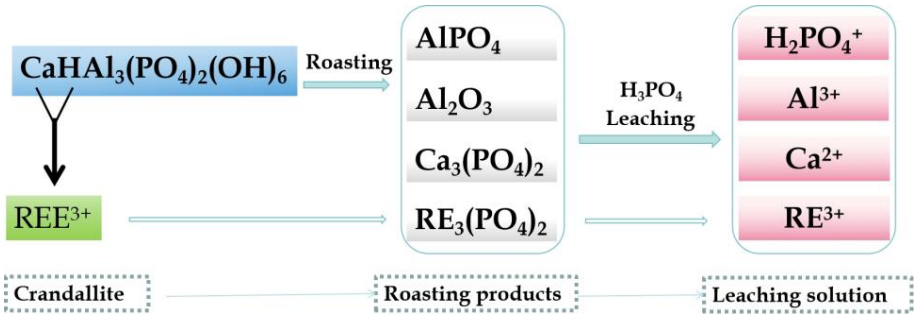

Fig. 18. Phase transformation of samples before and after roasting-leaching

5. Exploration of the separation / purification strategy

The composition of the leaching solution from roasting and phosphoric acid leaching is complex, mainly includes aluminium, calcium, and rare earth ions. The efficient extraction of REEs from leaching solutions has important theoretical value and practical significance.

Research has revealed that increasing the temperature can decrease the solubility of REEs in phosphoric acid (Wu et al., 2018). Thus, this study proposes that the recovery of Al^{3+} can be carried out initially by adjusting the pH, after which RE^{3+} can be precipitated and retrieved under heating conditions. Finally, concentrated sulfuric acid was added to remove Ca^{2+} and obtain phosphoric acid, achieving its recyclability.

6. Conclusions

This study has devised an efficient approach for the retrieval of REEs from svanbergite ores by roasting and phosphoric acid leaching. The effects of roasting-leaching conditions on the leaching recovery of REEs from svanbergite ores were investigated via RSM.

The optimum conditions for REE recovery were as follows: roasting temperature of 600℃, roasting time of 38.72 min, phosphoric acid concentration of 40%, leaching liquid/solid mass ratio of 10, leaching temperature of 75℃ and leaching time of 70 min, with a maximum predicted recovery of 83.57% for REEs. The most significant impact parameters were the roasting temperature, roasting time, phosphoric acid concentration, and the liquid–solid mass ratio of leaching solution. The leaching verification experiments revealed that the leaching recovery under the optimal conditions was 82.46%. The experimental values were close to the predicted values, confirming the model's accuracy and the feasibility of the optimized solution.

The mechanism analysis indicates that after the roasting process, the crandallite can generate new phases that subsequently dissolve in the phosphoric acid aqueous solution. The REEs mainly dissolve into the solution in the form of dihydrogen phosphates, thereby enabling the separation of REEs from the svanbergite ores. This study provides a valuable reference for the recovery of REEs from associated rare earth phosphate ores.

Acknowledgments

This research was supported by the [National Natural Science Foundation of China] Grant [41862002] and the [State Key Laboratory of Deposit Geochemistry, Institute of Geochemistry, Chinese Academy of Sciences] Grant [20180901]. The authors thank these funding institutions and also the reviewers and editors for their efforts.

References

AL-THYABAT, S., ZHANG, P., 2016. *Extraction of rare earth elements from upgraded phosphate flotation tailings*. Miner. Metal Proc., 33(1), 23-30.

AMINE, M., ASAFAR, F., BILALI, L., NADIFIYINE, M., 2019. *Hydrochloric acid leaching study of rare earth elements from moroccan phosphate*. J. Chem-NY., 2019(1), 4675276.

BATTSENGEL, A., BATNASAN, A., NARANKHUU, A., HAGA, K., SHIBAYAMA, A., 2018. *Recovery of light and heavy rare earth element-s from apatite ore using sulphuric acid leaching, solvent extraction and precipitation*. Hydrometallurgy, 179, 100-109.

CETINER, Z., 2003. *Experimental investigation of the solubility of the REE phosphate minerals monazite/xenotime and chloride complexation in hydrothermal solutions at 23 °C, 50 °C, 150 °C and saturated water vapor pressure*. University of Idaho. 77−90.

CETINER, Z., WOOD, S., GAMMONS, C., 2005. *The aqueous geochemistry of the rare earth elements. Part XIV. The solubility of rare earth element phosphates from 23 to 150 °C.* Chemical Geology, 217(1-2), 147-169.

CHENG, J., CHE, L., 2010. *The current situation and development trend of rare earth resource extraction in China*. Rare Earth, 31(02), 65-69.

DUAN, Q., SHEN, Z., SHU, L., ZHANG, Y., 1964. *Geological characteristics of a phosphorus deposit in Sichuan*. Geology in China, 04, 9-16.

FENG, Q., YANG, W., CHANG, M., WEN, S., LIU, D., 2024. *Advances in depressants for flotation separation of Cu-Fe sulfide minerals at low alkalinity: A critical review*. Int. J. Miner. Metal Mater., 31, 1–17.

GROUP, C., 2019. Phosphate rock waste: *A potential new source of rare earth elements.* Chemical Weekly, 38, 64.

HAMZAOUI, A., JAMOUSSI, B., M'NIF, A., 2008. *Lithium recovery from highly concentrated sol-utions: Response surface methodology (RSM) process parameters optimization.* Hydrometallurgy, 90(1), 1-7.

HUANG, S., 1977. *Report on comprehensive utilization test of svanbergite ore in Yanziya section of Qingping phosphate mine, Mianzhu, Sichuan Province* (3) - Electric heating method for refining yellow phosphorus, extracting aluminum, and recovering strontium and rare earth test report. Emei Institute of Mineral Resources Comprehensive Utilization.

HUANG, S., 1985. *Discussion on the wet comprehensive utilization of svanbergite ores*. Inorganic-Chemicals Industry. 09, 27-31.

HUANG, S., TANG, X., 1987. *Utilization pathways of svanbergite deposits in a certain area of China*. Journal of the Chinese Academy of Geological Sciences, 01, 234-239.

HUANG, X., ZHANG, Y., LI, H., 2011. The current situation and development trend of the development and utilization of rare earth resources in China. Bulletin of National Natural Science Foundation of China, 25(3), 134-137.

JIN H., WANG H., LI J., MAO X., ZHAO P., 2008. E*xperimental study on two flotation processes of rare earth-containing phosphate ore in Xinhua, Zhijin*. Guiyang: The National Academic Conference on Metallurgical Physical Chemistry in 2008.

LI, G., 1978. *Stage report on the comprehensive evaluation and research of the comprehensive utilization of svanbergite ore in Wangjiaping phosphate mine area, Mianzhu, Sichuan Province*. National Geological Data Museum.

LI, H., ZHANG, J., MAO, R., XIE, F., WANG, L., CHENG, J., 2023. *Selective extraction of rare earth elements from florencite rich sedimentary rare earth ore by sulfation.* Minerals Engineering, 202, 108294.

LI, L., ZHANG S., HE, Q., HU, X., 2015. *Application of response surface methodology in exper-imental design and optimization.* Research and Exploration in Laboratory, 34(08), 41-45.

LI, Z., XIE, Z., HE, D., DENG, J., ZHAO, H., LI, H., 2021. *Simultaneous leaching of rare ear-th elements and phosphorus from a Chinese phosphate ore using* H_3PO_4. Green Process. Synth., 10(1), 258-267.

LIANG, H., ZHANG, P., JIN, Z., DEPAOLI, D., 2017. *Rare-earth leaching from Florida phosphate rock in wet-process phosphoric acid production.* Miner. Metal Proc., 34(3), 146-153.

MA, K., ZHANG, J., DENG, Q., MEN, P., ZHANG, Y., SHI, X., 2022. *Study on REE occurrence in a svanbergite and basic ore characteristics.* Physicochem, Probl. Miner. Process., 58(3), 147377.

MONIR, M., NABAWIA, A., MOHAMMED A., 1999. *Recovery of lanthanides from Abu Tartur phosphate rock, Egypt*. Hydrometallurgy. 52(2), 199-206.

RLOAND, G., THOMAS, H., HARALD, S., and DIETRICH, 2000. *Compounds of the crandallite: materials from the earth on its way to technical applications.* Earth Science Frontiers. 7(002), 485-497.

SALEHI, S., NOAPARAST, M., SHAFAEI, S., AMINI, A., HEIDARNIA, A., 2015. *Iron leaching from bauxite ore in hydrochloric acid using response surface methodology.* Journal of Mining and Environment, 6(1), 103-108.

SUN, S., 1966. *Strontium aluminite phosphate sulfur and calcium bearing in sedimentary rocks*. Chin. J. Geol., 7(1), 22-31.

TANG, X., WANG, H., BAI, X., ZHANG, Y., 1982. *Semi-industrial test of alkaline medium flotation of svanbergite ore*. Multipurpose utilization of uineral resources. 04, 3-12.

WANG, J., 1991. *Processing and utilization of some low quality phosphate ores abroad.* Multipurpose Utilization of Mineral Resources., 06, 17-23.

WANG, S., JIANG B., LU R., 1986. *Calcination effect and agricultural evaluation of svanbergite ore in Sichuan*. Acta. Pedol. Sin., 23(4), 321-329.

WANG, S., XIA, P., 1988. *Study on the use of svanbergite as phosphorus fertilizer*. Soil and Fertilizers. 01, 5-9.

WANG S., 2018. Basic theory and process research on extraction of associated rare earths from phosphate ores. Northeastern University.

WENG, Z., JOWITT, S., MUDD, G., HAQUE, N., 2015. *A detailed assessment of global rare earth element resources: opportunities and challenges*. Econ Geol., 110(8), 1925-1952.

WU, J., ZHANG, W., JIANG, X., JIN, X., 2015. *Experimental study on rare earths separation f-rom Zhijin phosphate rock.* Phosphate and Compound Fertilizer, 30(04), 33-34.

WU, S., WANG, L., ZHAO, L., ZHANG, P., EL-SHALL, H., MOUDGIL, B., HUANG, X., ZHANG, L., 2018. *Recovery of rare earth elements from phosphate rock by hydrometallurgical processes–A critical review*. Chem Eng. J., 335, 774-800.

WU, S., ZHAO, L., WANG, L., HUANG, X., DONG, S., FENG, Z., CUI, D., ZHANG, L., 2018. *Dissolution behaviors of rare earth elements in phosphoric acid solutions.* Nonferrous Met. Soc. China., 28(11), 2375-2382.

WU, S., ZHAO, L., WANG, L., HUANG, X., CUI, D., 2019. *Simultaneous Recovery of Rare Ear-th Elements and Phosphorus from Phosphate rock by Phosphoric Acid Leaching and Selective Precipitation: Towards Green Process.* J. Rare Earth, 37(6).

YU, C., YING, J., LI, J., LI, Y., ZHOU, K., 2008. *Research on the production of phosphoric acid with svanbergite ore*. Industrial Minerals and Processing., 2, 7-10.

ZHENG, K., XIA, Y., WEN, X., LIU, Y., 2017. *Research progress on enrichment and extraction of rare earth elements from associated rare earth phosphate ores.* Conservation and Utilization of Mineral Resources., 05, 93-98.

ZHANG Q., ZHANG J., CHEN X., HAN J., 2003. *Selection of beneficiation process for rare earth-containing phosphate ore in Zhijin, Guizhou*. Metal Mine., 03, 23-25.

ZHANG, Y., ZHANG, J., WU, L., TAN, L., CHENG, J., 2021. *Extraction of lithium and aluminium from bauxite mine tailings by mixed acid treatment without roasting.* J. Hazard. Mater., 404(Pt B), 124044.